Line-focus probe excitation of Scholte acoustic waves at the liquid-loaded surfaces of periodic structures

A. G. Every
Department of Physics, University of the Witwatersrand, PO WITS 2050, South Africa

R. E. Vines and J. P. Wolfe
Department of Physics and Materials Research Laboratory, University of Illinois at Urbana-Champaign, Urbana, Illinois 61801
(Received 24 March 1999)

A model is introduced to explain our observation of Scholte-like ultrasonic waves traveling at the water-loaded surfaces of solids with periodically varying properties. The observations pertain to two two-dimensional superlattices: a laminated solid of alternating 0.5-mm-thick layers of aluminum and a polymer, and a hexagonal array of polymer rods of lattice spacing 1 mm in an aluminum matrix. The surface waves are generated and detected by line focus acoustic lenses aligned parallel to each other, and separated by varying distances. The acoustic fields of these lenses may be considered a superposition of plain bulk waves with wave normals contained within the angular apertures of the lenses. For homogeneous solids, phase matching constraints do not allow the Scholte wave to be coupled into with an experimental configuration of this type. This is not true for a spatially periodic solid, where coupling between bulk waves and the Scholte surface wave takes place through Umklapp processes involving a change in the wave-vector component parallel to the surface by a reciprocal lattice vector. In the experiments, the source pulse is broadband, extending up to about 6 MHz, whereas the spectrum of the observed Scholte wave is peaked at around 4 and 4.5 MHz for the layered solid and hexagonal lattice, respectively. We attribute this to a resonance in the surface response of the solid, possibly associated with a critical point in the dispersion relation of the superlattice. On rotating the solid about its surface normal, the Scholte wave displays dramatic variation in phase arrival time and, to a lesser extent, also group arrival time. This variation is well accounted for by our model. [S0163-1829(99)00539-1]

I. INTRODUCTION

Acoustic-wave propagation in periodically modulated structures has been studied for many years, and yet there are still interesting and challenging problems coming to light. The anomalous (supermodulus) elastic properties displayed by certain superlattices,[1] phonon transport through semiconductor superlattices in the high GHz frequency range[2] and sound attenuation by two-dimensional arrays of cylinders[3] are just a few of the areas attracting attention at the present time. Recently, there has been considerable interest in the optical properties of spatially periodic structures known as photonic crystals,[4] and this has led to questions being asked about analogous acoustic effects in phononic crystals.[5]

Wave propagation in infinite superlattices has been widely studied,[6,7] and a lot has been learned about surface waves on layered superlattices with the boundary parallel to the layers.[8] Only a beginning has, however, been made in the study of the surface wave properties of solids in which the periodic modulation occurs along, rather than perpendicular, to the bounding surface. On the theoretical front, Tanaka and Tamura[9] have recently reported illuminating calculations for surface waves on a square GaAs/AlAs superlattice.

The experimental investigations of Vines *et al.*[10,11] have brought to light the complex angular and frequency dependence of surface waves generated by a line-focus acoustic lens at the water-loaded surfaces of a number of two-dimensional (2D) superlattices that intersect the surface normally. The systems studied include a laminated solid of alternating layers of aluminum and a polymer,[12] and a hexagonal array of polymer rods in an aluminum matrix. Some of the effects observed in these experiments clearly display the dispersive effects of wave propagation through the superlattices, with lower frequency components in the region of 1 MHz predominating in the detected signals, even though the source spectrum extends up to about 6 MHz. A calculation of transverse wave propagation through an infinite superlattice is able to account partially for these features, as reported in Refs. 10 and 11.

The subject of the present paper is another type of observed feature, which is quite distinct in its behavior from the first two features. It is narrow band, peaked at 4 and 4.5 MHz for the layered solid and hexagonal lattice respectively, and its mean arrival time identifies it as being associated with a wave traveling along the surface at near to the speed of sound in water ($v = 1.48\ \mathrm{mm}/\mu\mathrm{s}$). This, and the fact that there is minimal attenuation of this wave with distance, indicates that the wave's energy flux is located predominantly in the water, and along the surface, suggesting a Scholte-like interfacial wave. The mechanism for the generation of this wave must, however, lie in the periodic modulation of the solid, firstly because of the frequency selectivity, and secondly to allow the incident bulk wave in the water to mode convert to a surface skimming wave (phase matching constraints prevent this for incidence on a homogeneous linear elastic solid). The most striking aspect of the feature is its angular dependence, observed when the sample is rotated about its surface normal. In this paper, we introduce a simple heuristic model that is successful in correlating the measured characteristics of the feature. The model highlights what are

probably the more important physical factors involved, and indicates the direction that a more fundamental theory of our observations might take. There is only one parameter in the model, which is the resonance frequency, and this we set equal to the observed frequency for each solid. Without further adjustment, the model gives a good account of the angular dependence of the feature for both superlattices, and also its dependence on the source receiver distance.

In Sec. II we briefly describe our experimental technique and the observed signals, with emphasis on the Scholte wave structure. In Sec. III we discuss a possible scenario for the origin of the resonant characteristic of the feature, and introduce a response function model that describes the means by which the acoustic signal can travel from the source lens to the receiver lens via a Scholte-like interfacial wave located mainly in the water. Sec. IV contains the comparison between theory and measurement.

II. EXPERIMENTAL SETUP AND MEASURED DATA

Full details of our method and measured data are published elsewhere[11,13–15] or are in press,[10] and so only a brief outline is given here. We discuss principally our observations of the Scholte-like waves at the water-loaded surfaces of two periodically modulated structures.

The first of these structures is a mutilayered solid of alternating 0.5 mm-thick layers of Al and a polymer,[12] giving a lattice period of $D=1.0$ mm. The surface of the sample on which the measurements are done is normal to these layers. The second sample is a 2D lattice of holes drilled in an Al substrate and filled with the same polymer. The lattice spacing, i.e., distance between neighbouring holes, is $a=1.0$ mm, and the polymer rods' filling fraction is 26%.

Our observations are carried out using a technique developed by some of us[13–15] to study the anisotropy of surface wave propagation in crystals and fiber composites. It employs a pair of cylindrical line focus acoustic lenses aligned parallel to each other and with their foci located on the surface of the solid a distance d apart [indicated by the lines T and R in Fig. 1(a)]. The one lens is the source of an ultrasonic pulse (T), and the other lens is the receiver (R). The incident pulse is of fairly short duration and consists of about two oscillations extending over ~ 0.5 μs, and with a bandwidth ranging between approximately 1 and 6 MHz. The lenses are tilted with their foci towards each other, to favor the generation and detection of partial waves whose wavevector components in the surface point from source to detector. To measure the angular dependence of the amplitude of the transmitted wave, the sample is rotated about an axis normal to the excitation surface.

Figure 2(a) shows the angle-time image that is obtained on the layered solid for a source to detector distance $d=5$ mm. The rotation angle θ is measured from the normal to the layers. Light and dark regions correspond to positive and negative amplitudes respectively. It is clear from the image that the time of flight and the transmittance of the various frequency components vary strongly with propagation angle. Our primary concern here is with the feature labeled A. The other two main features in this image, labeled B and C, are associated with wave transmission predominantly

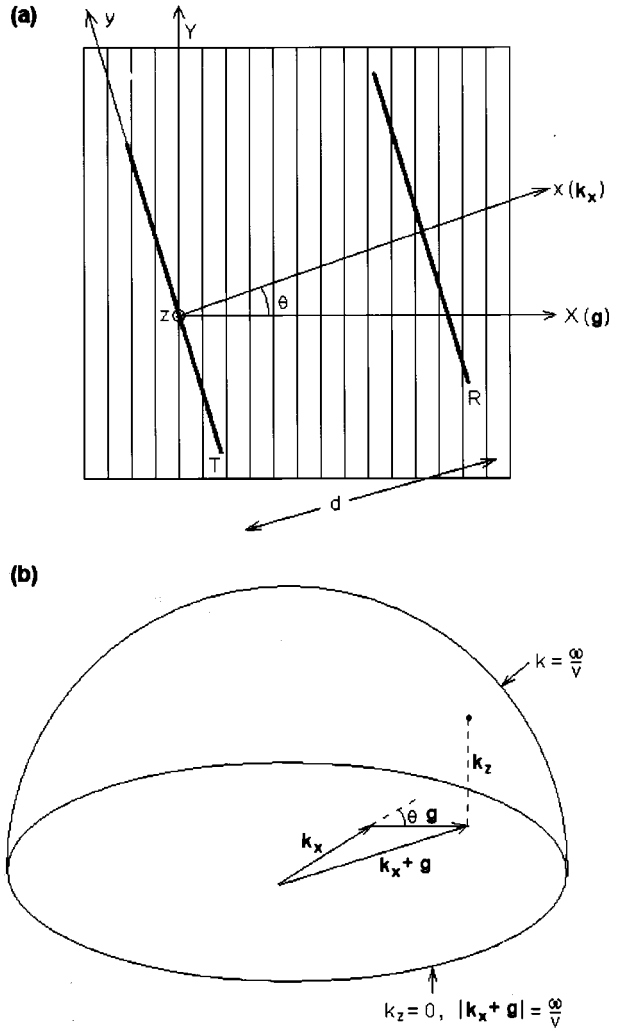

FIG. 1. (a) Experimental configuration and coordinate systems, (b) composition of wave vector in Umklapp process.

through the superlattice, and have been dealt with elsewhere.[10]

Feature A has some striking characteristics that distinguish it from the other features in the image. At least 6 complete, equally-spaced cycles can be discerned, corresponding to a narrow bandwidth peaked at a frequency $f \sim 4$ MHz, and with a $Q \sim 6$. When the higher frequency components of the source pulse are filtered out, feature A disappears, indicating that there is a resonance or resonant-like transmission mediated in some way by the periodic modulation of the solid.

The average propagation time of feature A is 3.3 μs in Fig. 2(a), and it increases proportionally as the source receiver separation d is increased (we have done measurements at $d=5$, 10, and 15 mm). This indicates a disturbance traveling along the surface with an average velocity of about 1.5 mm/μs, which is close to the speed of sound in water ($v=1.48$ mm/μs). Figure 2(b) shows the angle time image for $d=10$ mm. The mean arrival time for feature A is ~ 6.6 μs, which is double the value for the $d=5$-mm image. There is an additional feature D in this image, which is also associated with a resonance of some sort, but at a slightly lower frequency. The mean arrival time of this latter feature does not change significantly when d is varied, and we pre-

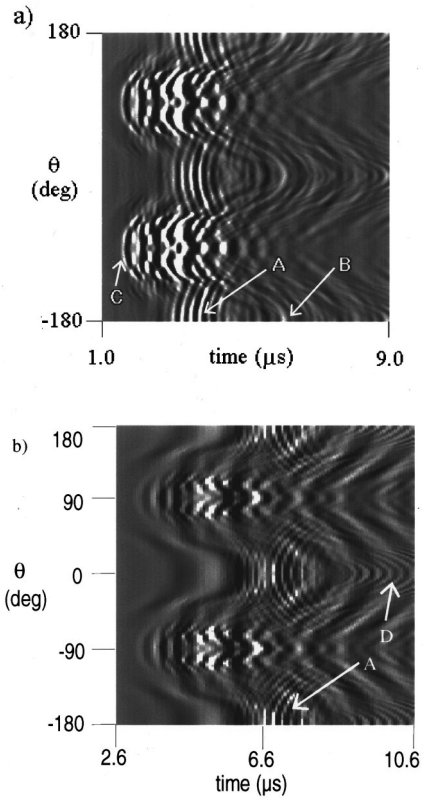

FIG. 2. Angle-time image showing the detected signal obtained on the layered solid for source to detector distance (a) $d=5$ mm, (b) $d=10$ mm. Our concern here is only with the features marked *A*.

sume it to be associated with a reflection of some sort, possibly from the back surface of the sample. We will not discuss feature *D* further in this paper.

The phase arrival times of the ripples are at a minimum for $\theta=0°$ (and $\pm 180°$), i.e., for wave propagation along the surface in a direction perpendicular to the layers. With change in θ, the phase arrival time τ for each arc-shaped ripple increases quadratically with θ, as accurately as can be determined, and the ripples gradually decrease in amplitude, eventually disappearing by about $\theta=45°$. We find that the phase delay time data for all the values of d we have carried out measurements at, can be fitted to the empirical Eq. (1), with coefficients $\alpha(d)$ given in the second column of the table below

$$\tau(d,\theta)=\alpha(d)\,\theta^2, \tag{1}$$

d(mm)	$\alpha(d)$ μs/rad^2	$\alpha_{theory}(d)$ μs/rad^2
5	0.26	0.39
10	0.74	0.78
15	1.19	1.17

Between 10 and 15 mm, the variation of the coefficient $\alpha(d)$ is almost proportional to d, but the value of $\alpha(5)$ lies somewhat below its interpolated value. This may have to do with the fact that for small d, the focal regions of the two lenses begin to overlap. The third column in the table above lists the theoretical values of $\alpha(d)$ to be discussed later.

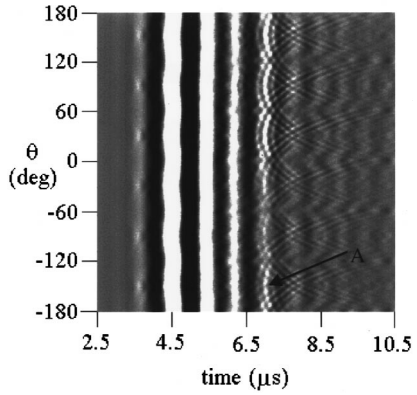

FIG. 3. Angle-time image obtained on the hexagonal superlattice with source to detector distance $d=10$ mm.

Examination of Fig. 2(b) reveals that there is need to distinguish between the phase arrival time discussed above, and the group arrival time of the wavepacket of ripples. The latter has a somewhat weaker angular dependence than that of the phase arrival time, which is evident from the fact that the late arriving ripples fade somewhat sooner with increasing θ, and in their place some early arrival ripples begin to build up. It is difficult to measure the group arrival time variation accurately; we estimate it to be about a factor of two smaller than that of the phase arrival time.

The experimental angle-time image for the hexagonal lattice with $d=10$ mm is shown in Fig. 3. Again, it is only the feature *A* (the set of fine intersecting arced lines between 6.5 and 9.5 μs) that is of concern to us here, the other features being associated with wave propagation through the superlattice as reported elsewhere. In contrast to the other features in this image, the *A* waves are much higher in frequency, in the region of 4.5 MHz, and they have an average velocity close to the sound speed in water. For this system, the angular dependence of the waves can be followed out to almost 90° on either side of the minimum arrival time directions, which lie midway between adjacent nearest neighbor directions. The pattern repeats itself after 60°, which is to be expected in view of the six-fold rotational symmetry of the lattice, and as a consequence each set of arced ripples intersects with its neighboring sets of ripples at an angular distance of 30°, with its next neighboring sets of ripples at 60°, and even perceptibly with the following set at 90°.

For small θ, the angular dependence of the phase delay time of the ripples is given quite accurately by

$$\tau=\alpha\theta^2, \quad \alpha=0.77\ \ \mu\text{s/rad}^2, \tag{2}$$

but for larger θ the variation departs from simple quadratic dependence on θ. Figure 4 shows the measured variation of τ compared with the quadratic fit to the small angle data and with the theoretical prediction to be described later. The distinction between phase and group arrival time is more marked for the hexagonal lattice, in the way that, with increasing θ, new early arrival ripples grow and late arriving ripples disappear. An estimate puts the variation of the group arrival time with θ at about half of that of the phase arrival time.

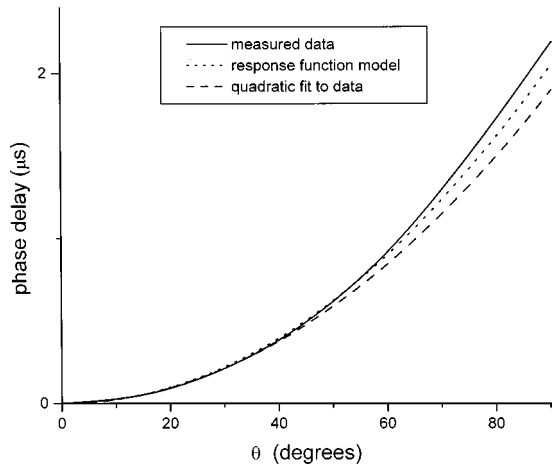

FIG. 4. Comparison between measured and calculated variation of the phase delay time τ for the hexagonal lattice and $d=10$ mm.

III. RESPONSE FUNCTION MODEL

A. Resonance response of solid

The first question we address here is why the *A* feature is so much sharper in frequency than the source pulse. Providing a definitive answer to that question will probably require an accurate calculation of the surface dynamic response function of the water-loaded periodic solid.[16] This is a worthy goal, but lies outside the scope of the present study. Rather we suggest here a plausible scenario for the origin of the observed resonance.

Well away from the bounding surface, the vibrational modes of the superlattice are Floquet waves that can be ascribed a wave vector $\mathbf{k}$ confined to the first Brillouin zone, and whose frequencies are given by a dispersion relation $\omega_n(\mathbf{k})$, where n is the band index. In the case of the layered solid, taking the X direction normal to the layers, $k_X \in \{-g/2, g/2\}$, where $g=2\pi/D$ is the recriprocal lattice ''vector,'' and k_Y and k_Z are unbounded. For the hexagonal lattice, with the Z-direction along the rods, the reciprocal lattice is hexagonal with lattice spacing $g=4\pi/\sqrt{3}a$ and rotated by 30° with respect to the real lattice, and (k_X, k_Y) is contained within the first Brillouin zone, while k_Z is unbounded. We will also make use of a coordinate system (x,y,z) obtained from (X,Y,Z) by rotation through angle θ about the $Z(z)$ axis [see Fig. 1(a)].

For both types of lattices there are critical points $\mathbf{k}=\mathbf{k_0}$ where $\omega_n(\mathbf{k})$ is stationary.[17] These generically occur at the center of the Brillouin zone ($\mathbf{k}=0$), and at the centers of the zone boundaries. If we assume the source and detector to be infinitely long and aligned along the y direction, which is inclined at an angle θ to the structural Y axis of the sample, [see Fig. 1(a)], we are dealing essentially with two dimensional waves with no component k_y. A critical point may thus be a maximum or a minimum in the frequency, in which case the frequency distribution function $\rho(\omega)$ has a discontinuity at $\omega_0=\omega_n(\mathbf{k_0})$, or it could be a saddle point, in which case $\rho(\omega)\sim \ln|\omega-\omega_0|$, diverging logarithmically at ω_0.[17]

Further, the modes with $\mathbf{k}$'s in the vicinity of a critical point have vanishingly small group velocities, $\mathbf{V}=\partial\omega/\partial\mathbf{k}$, and so energy injected into these modes moves only slowly away from the source. With the superlattice terminated by a surface normal to the z direction, k_z is no longer a conserved quantity. Nevertheless, the existence of a critical point in the bulk wave dispersion relation will have a profound effect on the surface dynamical response of the solid. A force distributed uniformly along the y axis and with frequency near ω_0 for a saddle point, will have a high density of modes in the bulk that it can couple to, and since these modes cannot readily remove their vibrational energy from the surface, there will be a buildup of energy near the surface. Thus, the surface will be observed to respond with large amplitude when excited at or near that frequency.

Consider now the water in contact with the surface of the solid. It will certainly have a damping effect on the resonant surface response, but this will be small if the acoustic mismatch between the liquid and the solid is large and the solid and liquid are only weakly coupled. The more important role of the liquid, in the first instance, is that it is the transmission medium through which the force is delivered to the surface. The incident pressure field in the focal plane of the source lens is, on the basis of the angular spectrum method, represented by the superposition of plane waves

$$p_0(x,t)=\int dk_x d\omega \mathcal{F}(k_x,\omega)\exp\{i(k_x x-\omega t)\} \qquad (3)$$

where the spectrum $\mathcal{F}(k_x,\omega)$ extends over a fairly broad range of spatial and temporal frequencies. The spread is, however, confined to positive values of k_x/ω because of the tilting of the lens, and there is not much loss of generality in considering only positive k_x and ω. Each partial wave gives rise to a spatially and temporally periodic normal force on the solid's surface and, in response to this force, there are a set of surface displacements (we consider only the normal components) $G(\mathbf{k}_x, \mathbf{k}_x+\mathbf{g}, \omega)$. The surface responds at the same frequency ω, but because of the periodic modulation of the elastic properties of the solid, there are surface displacements with wave vectors $\mathbf{k}_x+\mathbf{g}$, $(\mathbf{k}_x=k_x\hat{\mathbf{x}})$ for all reciprocal lattice vectors $\mathbf{g}$, including 0. For a homogeneous solid, there is no periodicity or dispersion, and G collapses to $G(k_x/\omega)$ for a particular direction.

Bearing in mind the flatness of the bulk wave dispersion relation near a critical point, and the resonant form expected for the response, we will suppose that G for a reciprocal lattice vector $\mathbf{g}$ of interest, has the simple harmonic oscillator form coresponding to a frequency ω_0. Restricting attention to positive frequencies not far removed from ω_0, where the influence of the negative frequency resonance is small, it follows that

$$G(\mathbf{k}_x, \mathbf{k}_x+\mathbf{g}, \omega)\sim \frac{1}{\omega_0-\omega-i0_+}. \qquad (4)$$

B. Response of the water

Our experiments are conducted with an acoustic barrier strategically placed so that specularly reflected waves, without considerable lateral displacement, are not detected by the receiver lens. We seek the interpretation of feature *A*, therefore, in a pressure wave in the water, which travels along the solid's surface. Were the solid perfectly rigid, then a plane sound wave in the liquid traveling parallel to the surface

would satisfy the boundary conditions (ignoring the effects of viscosity). The finite compliance of the solid reduces the velocity of this wave, and causes it thereby to separate from the continuum of bulk sound waves in the liquid and become a true interfacial wave, falling off exponentially with distance from the interface. This is the Stoneley-Scholte interfacial wave. The wave also extends into the solid, but the amplitude of this latter part and the energy flux associated with it, will be minimal if the acoustic mismatch is large. In that case the speed of this wave will also not differ much from the sound speed in water, v. In this marginal situation, it is difficult to resolve the true Scholte wave from a peak in the density of bulk mode slownesses $s_x = k_x/\omega$ at the limiting slowness $s_x = 1/v$. See Refs. 16 and 18 for more extensive discussions of this point. From an experimental point of view, faced with limited velocity resolution, we are therefore, for our particular system, justified in talking of a somewhat loosely defined Scholte-like wave traveling in the water along the surface of the solid at speed v.

Backtracking a moment, we arrived in the last section at the idea of the surface of the solid vibrating with wave vector $\mathbf{k}_x + \mathbf{g}$ and frequency ω. This will give rise to an external pressure disturbance on the liquid with those spatial and temporal frequencies. If $|\mathbf{k}_x + \mathbf{g}| < \omega/v$, then phase matching in the surface is achieved with a wave in the liquid having real $k_z = \sqrt{\omega^2/v^2 - |\mathbf{k}_x + \mathbf{g}|^2}$ [see Fig. 1(b)], which is a bulk wave that radiates energy away from the surface. For $|\mathbf{k}_x + \mathbf{g}| \gg \omega/v$, on the other hand, k_z is large and imaginary and there is no radiation at all. The condition for radiation of energy into a Scholte-like surface mode is

$$|\mathbf{k}_x^0 + \mathbf{g}| \approx \omega/v. \tag{5}$$

For $\mathbf{g}$ inclined at an angle θ to the x direction,

$$|\mathbf{k}_x^0 + \mathbf{g}|^2 = (k_x^0 + g\cos\theta)^2 + g^2 \sin^2\theta. \tag{6}$$

Taking k_x and ω both to be positive and not too far from satisfying the resonance condition, the response function for the liquid pertaining to surface wave excitation is

$$G'(\mathbf{k}_x + \mathbf{g}, \omega) \sim \frac{1}{k_x^0 - k_x + i0_+}, \tag{7}$$

where, from Eqs. (5) and (6),

$$k_x^0(\omega, \theta) = \sqrt{\frac{\omega^2}{v^2} - g^2 \sin^2\theta} - g\cos\theta. \tag{8}$$

C. The propagating disturbance

Now, combining the original source field, the solid's response and the response of the liquid, we have a wavefield $p(x,t)$ propagating in the liquid along the surface given by

$$p(x,t) = \int dk_x d\omega \mathcal{F}(k_x, \omega) \exp\{i(k_x x - \omega t)\} \times G(\mathbf{k}_x, \mathbf{k}_x + \mathbf{g}, \omega) G'(\mathbf{k}_x + \mathbf{g}, \omega). \tag{9}$$

The field is able to be detected by the receiver lens because the periodic modulation of the solid provides also the mechanism for the reradiation of the surface wave into this lens. Taking the spectrum $\mathcal{F}(k_x, \omega)$ to be constant, and the forms postulated for the response functions above, we have that

$$p(x,t) = \int dk_x d\omega \exp\{i(k_x x - \omega t)\} \times \frac{1}{\omega_0 - \omega - i0_+} \frac{1}{k_x^0 - k_x + i0_+}. \tag{10}$$

On integrating with respect to k_x and then to ω, this yields the result

$$p(x,t) \sim \Theta\{x\} \Theta\left\{ t - \left.\frac{\partial k_x^0}{\partial \omega}\right|_{\omega_0} x \right\} \exp i[k_x^0(\omega_0, \theta)x - \omega_0 t], \tag{11}$$

where Θ is the Heaviside step function.

The essential features of this derivation are the existence of a well-defined resonance and an Umklapp process that allows an incident k vector to couple to a larger $k_\parallel$ surface wave. In the final analysis, it is Eq. (11) that we regard as containing the essence of our model. It gives a good account of our experimental results, and can stand alone as a phenomenological description of those results.

IV. COMPARISON BETWEEN THEORY AND EXPERIMENT

Equation (11) can be interpreted physically as follows. The factor $\Theta\{x\}$ pertains to the forward propagation of the disturbance, in the positive x direction, and has arisen from the restriction of k_x and ω to both being positive. This, as mentioned earlier, is tied up with the tilting of the source lens in the experiments. The second factor $\Theta\{t - \partial k_x^0/\partial\omega|_{\omega_0} x\}$ describes the delay of the wavepacket in reaching the detector. To encompass also the subsequent fall off in the signal amplitude with time, the damping in Eq. (10) would need to be finite. The phase factor $\exp i[k_x^0(\omega_0, \theta)x - \omega_0 t]$ describes the ripples and how they are time shifted as θ is changed.

The variation in the phase delay time of the ripples with θ, setting $x = d$, is given by

$$\tau = [k_x^0(\omega_0, \theta) - k_x^0(\omega_0, 0)]d/\omega_0, = \frac{d}{v}\{\sqrt{1 - \beta^2 \sin^2\theta} - \beta\cos\theta + \beta - 1\}, \tag{12}$$

where $\beta = gv/\omega_0$. For small θ, this approximates to

$$\tau = \alpha_{theory}\theta^2, \tag{13}$$

$$\alpha_{theory} = \frac{d\beta(1-\beta)}{2v}. \tag{14}$$

Similarly, the group arrival time and its variation with θ is given by

$$\tau_{group} = \left.\frac{\partial k_x^0}{\partial \omega}\right|_{\omega_0} d, \tag{15}$$

which, for small θ, approximates to

$$\tau_{group}=\frac{d}{v}\left\{1+\frac{1}{2}\beta^2\theta^2\right\}. \tag{16}$$

For $\theta=0$, $\tau_{group}=d/v$, the time it takes the wavepacket to travel directly from the source to the detector at the sound speed in water. For $\theta\neq 0$, the energy flux direction is tilted away from the forward direction, and the group arrival time is extended.

In fitting the angular dependences, the only adjustable parameter there is in the above expressions is ω_0 (or equivalently β). We will not treat this as a free parameter, but rather set it equal to the observed frequency of feature *A* in the angle-time images, which is 4 MHz for the layered solid and 4.5 MHz for the hexagonal lattice.

Thus, for the layered solid, taking $g=2\pi/D=2\pi$ mm^{-1}, $\omega_0=8\pi$ μs^{-1}, and $v=1.5$ mm/μs, we arrive at the theoretical values for the coefficients $\alpha_{theory}(d)$ listed below Eq. (1). The values of α for $d=10$ and 15 mm are in very good agreement with measurement, but the measured value of α for $d=5$ mm lies somewhat below the calculated value, possibly because the focal regions of the two lenses begin to overlap at short distances and there is a specularly reflected component to the detected signal which does not vary with θ. The coefficents of θ^2 in the group arrival times, $d\beta^2/2v$, are 60% of the values of $\alpha_{theory}(d)$, which is consistent with observation.

For the hexagonal lattice, taking $g=4\pi/\sqrt{3}a=4\pi/\sqrt{3}$ mm^{-1}, $\omega_0=9\pi$ μs^{-1}, and $d=10$ mm, the calculated value of α comes out to be 0.79 μs/rad^2, which is close to the measured value of 0.77 μs/rad^2. For the full range of θ up to 90°, in which the deviation from quadratic dependence does become noticeable, the variation of τ is shown graphically in Fig. 4. As can be seen, the agreement between theory and measurement is good. The coefficient of the quadratic dependence of the group arrival time is calculated to be 0.40 μs/rad^2, which is about 50% of the value of α_{theory}, and is consistent with observation.

V. SUMMARY AND CONCLUSIONS

We have shown how a Scholte-like wave can be generated by the use of a line focus acoustic lens to insonify the surface of a solid whose properties are periodically modulated along the surface. This modulation relaxes the normal phase matching constraints that prevent mode conversion of bulk waves to surface waves. The heuristic model we have invoked accounts well for our data measured on a layered solid and an hexagonal array of polymer rods in an Al matrix. Our model consists essentially in an ansatz about the response of the system pertaining to the generation of Scholte-like waves. The periodicity of the solid is presumed to be the origin of the resonant frequency that is observed, and it is also the means by which an incident bulk wave in the liquid mode converts to a surface wave via an Umklapp process involving a change in the wave-vector component parallel to the surface. The model is able to account quantitatively for the angular dependence of our measured Scholte wave data and its variation with source receiver separation.

A more fundamental theory for the systems we have been describing is desirable. It would presumably be an extension of the type of analysis carried out by Tanaka and Tamura,[9] with liquid loading included, and the reflectivity or response function calculated.

There are potential applications of bounded superlattices in acoustic beam manipulation, filtering, sound abatement and other areas.

ACKNOWLEDGMENTS

This work was supported in part by the Department of Energy Grant No. DEFG02-96ER45439 in the Frederick Seitz Materials Research Laboratory. A.G.E. acknowledges the hospitality of the Physics Department of the University of Illinois at Urbana-Champaign.

[1] See, e.g., R. Cahn, Nature (London) **324**, 108 (1986); E.E. Fullerton, I.K. Schuller, F.T. Parker, K.A. Svinarich, G.L. Eesley, R. Bhadra, and M. Grimsditch, J. Appl. Phys. **73**, 7370 (1993), and papers cited therein.

[2] S. Tamura, D.C. Hurley, and J.P. Wolfe, Phys. Rev. B **38**, 1427 (1988).

[3] J.V. Sanchez-Perez, D. Caballero, R. Martinez-Sala, C. Rubio, J. Sanchez-Dehesa, F. Meseguer, J. Llinares, and F. Galuez, Phys. Rev. Lett. **80**, 5325 (1998).

[4] J.D. Joannopoulos, R.D. Meade, and J.N. Winn, *Photonic Crystals* (Princeton University Press, Princeton, 1995).

[5] Phys. Today **52** (1), 9 (1999); see also Ref. 3.

[6] M.S. Kushwaha *et al.*, Phys. Rev. B **49**, 2313 (1994); M.S. Kushwaha and P. Halevi, Appl. Phys. Lett. **64**, 1085 (1994).

[7] M. Sigalas and E.N. Economou, Solid State Commun. **86**, 141 (1993).

[8] T. Aono and S. Tamura, Phys. Rev. B **58**, 4838 (1998).

[9] Y. Tanaka and S. Tamura, Phys. Rev. B **58**, 7958 (1998).

[10] R.E. Vines, A.G. Every, and J.P. Wolfe, Phys. Rev. B (to be published).

[11] R.E. Vines, Ph.D. thesis, University of Illinois at Urbana-Champaign, 1998.

[12] Crystalbond^{TM} 509 from Aremco Products.

[13] R.E. Vines, S. Tamura, and J.P. Wolfe, Phys. Rev. Lett. **74**, 2729 (1995).

[14] R.E. Vines, M.R. Hauser, and J.P. Wolfe, Z. Phys. B **98**, 255 (1995).

[15] J.P. Wolfe and R.E. Vines, Proc.-IEEE Ultrason. Symp. **96**, 607 (1996).

[16] A.G. Every and G.A.D. Briggs, Phys. Rev. B **58**, 1601 (1998).

[17] A.A. Maradudin, E.W. Montroll, G.W. Weiss, and I.P. Ipatova, in *Theory of Lattice Dynamics in the Harmonic Approximation*, edited by F. Seitz and D. Turnbull, Solid State Physics, Supplement 3 (Academic Press, New York, 1971).

[18] X. Zhang, J.D. Comins, A.G. Every, P.R. Stoddart, W. Pang, and T.E. Derry, Phys. Rev. B **58**, 13 677 (1998).